

New solar twins and the metallicity and temperature scales of the Geneva Copenhagen Survey ^{*}

Juliet Datson^{1†}, Chris Flynn^{2,3,4} and Laura Portinari¹

¹*Tuorla Observatory, Department of Physics and Astronomy, University of Turku, Finland,*

²*Department of Physics and Astronomy, University of Sydney, NSW 2006 Australia*

³*Finnish Centre for Astronomy with ESO, University of Turku, FI-21500, Piikkiö, Finland*

⁴*Centre for Astrophysics and Supercomputing, Swinburne University of Technology, VIC 3122 Australia*

Accepted 2012 July 16. Received 2012 July 2; in original form 2012 February 17

ABSTRACT

We search for “solar twins” in the Geneva-Copenhagen Survey (GCS) using high resolution optical spectroscopy. We initially select Sun-like stars from the GCS by absolute magnitude, $(b - y)$ colour and metallicity close to the solar values. Our aim is to find the stars which are spectroscopically very close to the Sun using line depth ratios and the median equivalent widths and depths of selected lines with a range of excitation potentials. We present the ten best stars fulfilling combined photometric and spectroscopic criteria, of which six are new twins.

We use our full sample of Sun-like stars to examine the calibration of the metallicity and temperature scale in the GCS. Our results give rise to the conclusion that the GCS may be offset from the solar temperature and metallicity for sun-like stars by 100 K and 0.1 dex, respectively.

Key words: stars: abundances – stars: fundamental parameters – stars: solar-type

1 INTRODUCTION

“Solar twins” (or “solar analogues”) are stars which are very close matches to the spectroscopic and photometric properties of the Sun (Cayrel de Strobel 1996), and while there is currently no “perfect twin”, a few stars are known which are very close matches to the Sun. For over a decade, the star considered most similar to the Sun has been 18 Sco/HD 146233 (Porto de Mello & da Silva 1997; Soubiran & Triaud 2004), and recent asteroseismological and interferometric measurements have confirmed its radius and mass to be solar within a few percent (Bazot et al. 2011). Based on its spectroscopic properties, HD 98618 was considered the next best solar twin by Meléndez et al. (2006), while Takeda et al. (2007) have found HIP 100963 to be as good a twin as 18 Sco (although both stars have a higher Li abundance than the Sun by 0.5 and 0.8 dex respectively). Currently, HD 56948 is the star considered closest to the Sun (Meléndez & Ramírez 2007) – its lithium abundance is very similar to the Sun, and together with another close twin (HIP 73815), it shows that the solar lithium abundance

is not atypical. Some tens of solar twins (or solar analogues) have been published in recent years (Takeda et al. 2007; Meléndez et al. 2009); and a solar twin has even been identified in the open cluster M67 (Önehag et al. 2010). To date all solar twins show small but interesting differences with respect to the Sun: such as the lithium abundance being high (Meléndez et al. 2006) or the stars being variable and showing chromospheric activity (e.g. 18 Sco, Hall & Lockwood 2000).

Solar twins are useful because, obviously enough, one cannot point the same instruments/telescopes at the Sun as used on faint objects in the night sky. This gives rise to a major difficulty with calibrating the stellar metallicity and temperature scale to the same scale as the Sun, in which these parameters are measured (notwithstanding that the absolute solar metallicity has been under considerable discussion in the last decade, Asplund et al. 2009).

The largest extant sample of solar type stars (F, G and K dwarfs), the Geneva-Copenhagen-Survey (hereafter GCS, Nordström et al. 2004), has a photometric metallicity and temperature scale which is tied to the stellar colours. Recently, the metallicity and temperature calibrations have been called into question by Casagrande et al. (2010), who used the InfraRed Flux Method on 423 stars, and the properties of 10 solar twins, to argue that the GCS scale may need shifting by about 100 K in temperature and 0.1 dex in

^{*} Based on observations made with ESO Telescopes at the La Silla Observatory under programme ID 077.D-0525 and from the ESO Science Archive Facility under request number JDATSHC-CCA119545 and following.

† E-mail: juliet.datson@utu.fi

metallicity. We address this topic in this paper, presenting a new method for testing the scales in the GCS catalogue using solar analogues, and finding a similar shift.

Interest has revived in solar twins since the advent of exoplanet detection. Interestingly, the first discovered exoplanet host, 51 Peg (Mayor & Queloz 1995), is a very good solar twin (Cayrel de Strobel 1996). Exoplanets have been found around other solar twins (Endl et al. 2005; Udry et al. 2007), but to date no systematic searches have been undertaken. One of our aims is to provide a list of nearby solar twins by searching systematically for them in the GCS.

Recently Meléndez et al. (2009) and Ramírez et al. (2009) have suggested that whether a star hosts exoplanets or not might be revealed in the detailed chemical composition obtained from high resolution spectra. Another motivation for this study is to provide new targets to probe this correlation further.

In this paper we present the results of our own quest for solar twins, based on photometric selection from the GCS catalogue, combined with high resolution spectroscopic data. Most previous surveys looking for solar twins have focused on objects of the Northern Hemisphere, such as at the Observatoire des Haute Provence (Soubiran & Triaud 2004), Keck (Meléndez et al. 2006; King et al. 2005) or the McDonald Observatory in Texas (Ramírez et al. 2009). We explore the relatively understudied Southern Hemisphere from the Max-Planck-Gesellschaft (MPG)/European Southern Observatory (ESO) 2.2m at La Silla Observatory, giving us the opportunity to extend our search to targets not considered previously, and we turn up with six new twins.

In this paper we provide a description of our photometric candidate selection process in section 2; in section 3 we outline the observations and data reduction; in section 4 we present our methods for finding solar twins and the results. In section 5 we use our full spectroscopic sample of about a hundred Sun-like stars to test the temperature and metallicity scale in the GCS, by differential comparison to the solar spectrum, and we draw our conclusions in section 6.

2 CANDIDATE SELECTION

Our candidate solar-twins were selected from the first release of the Geneva-Copenhagen-Survey (GCS-I) (Nordström et al. 2004) of Stromgren colours, absolute magnitudes, metallicity and temperature estimates for ~ 14000 nearby F to K type stars. We selected stars bracketing the solar ($b - y$) colour, absolute visual magnitude M_V and metallicity, for which we adopt the solar values of $(b - y)_\odot = 0.403$ (Holmberg et al. 2006), $M_V = 4.83$ (Allen 1976) and $[\text{Fe}/\text{H}] = 0.0$ (by definition). Our ranges are : $0.371 < (b - y) < 0.435$, in absolute magnitude $4.63 < M_V < 5.03$ and in metallicity (GCS-I scale) $-0.15 < [\text{Fe}/\text{H}] < 0.15$. These criteria resulted in 338 stars, of which 80 were chosen for the proposal as accessible from La Silla, and not already available in the Fiber-fed Extended Range Optical Spectrograph (FEROS) archive. In the end, 70 of these 80 targets were observed (all in service mode).

In Fig. 1 we show the colour-magnitude diagram (CMD) of the main sequence and turnoff stars from the GCS-I catalogue. The dots show our initial photometric twin candi-

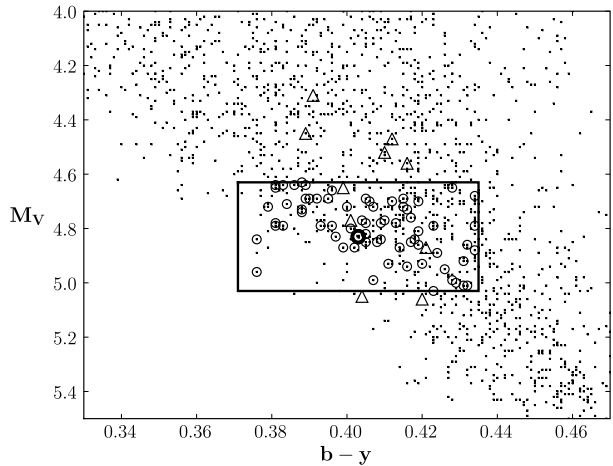


Figure 1. Stars from the Nordström et al. (2004) catalogue (GCS-I) (dots), in the metallicity range of $-0.15 < [\text{Fe}/\text{H}] < 0.15$, together with our initial twin candidates (circles) and the candidates from Soubiran & Triaud (2004) (triangles). The Sun is marked in the middle of the box. The solar twin candidates of the Soubiran & Triaud (2004) sample (triangles) tend to lie redward (cooler) and tend to be intrinsically brighter than the Sun.

dates, chosen for spectroscopic follow-up. An interesting effect appears if we show the 10 very good spectroscopically matched solar twins found by Soubiran & Triaud (2004) (triangles). Their twins tend to lie redward (cooler) and tend to be brighter than the Sun. This highlights the point (concluded by those authors) that purely spectroscopic matching might still yield stars with systematic differences to the Sun in other properties – thus, in this paper, we examine the effects of using both spectroscopic and photometric criteria to find solar twins.

While this project was being undertaken, two revisions of the Geneva-Copenhagen Survey (GCS-II and GCS-III) (Holmberg et al. 2007, 2009) were published. Both revisions addressed the metallicity, age and temperature scales of the stars, and utilised the updated Hipparcos parallaxes (van Leeuwen 2007) when they became available. This resulted in increased temperatures, which went up by an average of 80 K at solar values and in decreased metallicities, which went down by an average of 0.05 dex.

With the revised absolute magnitudes and metallicities, some of our target stars moved slightly out of the original selection window while others moved in. These new arrivals have been included in our sample, as we searched the FEROS archive at ESO and found spectra for 28 of these candidates. We also included stars in our sample which have been classified as ‘Sun-like’ stars by others (Sousa et al. 2006; Takeda et al. 2007; Hall et al. 2009; Ramírez et al. 2009; Soubiran & Triaud 2004). This yielded another 47 stars, bringing our total sample to 145 objects. They range in apparent V magnitudes from 3.5 to 9, with the majority lying around $V = 8$.

Fig. 2 shows our final spectroscopic sample in the M_V vs. $(b - y)$ plane. Our basic candidate stars, initially selected from the GCS-I, but with revised GCS-III data and stars which entered the selection window as a result of the revised

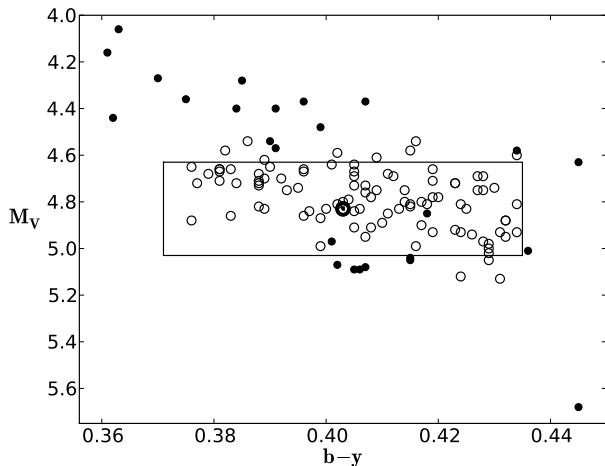


Figure 2. As Fig. 1, showing our target sample as open circles (from GCS-I and GCS-III) and the targets taken from other papers (filled circles). The Sun is shown in the middle of the box, which represents our original selection window.

GCS data, are shown as open circles. Finally, Sun-like stars from other studies in the literature are shown as filled circles. The Sun’s location is shown in the middle of our selection box.

Some stars selected from the literature lie very far in absolute magnitude and colour from our selection window. This is because often the authors adopted a broad definition of Sun-like stars, sometimes extending to F and K dwarfs (Takeda et al. 2002) or metal-rich stars (Sousa et al. 2006). We decided to keep all those stars in our analysis, to have a chance to test broad trends with temperature and metallicity in the spectroscopic selection of our best twin candidates.

3 OBSERVATIONS

Spectra of 70 of our 80 target stars were obtained with the FEROS instrument (Kaufer et al. 1999) on the MPG/ESO 2.2 meter telescope at La Silla, Chile. FEROS is an echelle spectrograph with a resolution of $R \sim 48000$ and covers a spectral range of 3500-9200 Å, permitting the analysis of a wide range of lines. Spectra were obtained in service mode over the period 77A, in July and August 2006. Exposure times varied from 200 s up to 950 s (depending on object magnitude), resulting in typical signal to noise (S/N) ratios of ~ 100 -150.

We also obtained spectra from the FEROS archive if they had exactly the same instrumental setup as our service observations, resulting in an additional 75 stars. These spectra were taken between 2003 to 2008. We have checked, by means of twilight spectra and repeated observations of τ Ceti from the archive, and found that the instrument is very stable over these long time scales (details are in section 4.5). The S/N for these additional spectra are also of the order of 100-150. High S/N spectra of the asteroid Ceres were also taken as our solar spectrum comparison.

Data reduction was done with the FEROS pipeline, resulting in 1-D spectra that were flatfielded, bias subtracted, sky subtracted and wavelength calibrated in the

range of 3500-9200 Å. The wavelength calibration is based on ThAr+Ne arcs and the pipeline rebins the spectra to a linear 0.03 Å resolution over their full wavelength range.

The final FEROS pipelined spectra contained a number of significant wiggles in the continuum level over short and long scales. These were far too complex to remove using polynomial or spline fits over the whole spectral range. We took the simple approach of fitting piecewise 10 Å sections of the spectrum, and normalising to the mode of the histogram of pixel values in each section. This procedure produced very flat spectra in regions with few or weak lines (i.e. most of the spectrum). All the lines analysed were in regions with only a few weak lines, and this simple procedure was found to be entirely adequate. Stars for which we had several spectra showed that this procedure was also very stable.

During the reduction process we found some spectra to be too noisy to be flattened properly and some spectra with unaccountable continuum jumps. These spectra were discarded, reducing our sample to 100 stars.

4 ANALYSIS

A number of approaches have been adopted to finding solar twins by groups active over the last decade. These are : χ^2 matching over a large range in the spectral energy distribution (SED) (Soubiran & Triaud 2004); comparison of the equivalent widths of specific iron lines relative to the Sun, (Takeda et al. 2002; Meléndez & Ramírez 2007); comparison of the line depth of specific iron lines (Meléndez et al. 2006) or line-by-line differential abundance comparison (Önehag et al. 2010). In this paper we apply four methods to our sample with the view that good twins should stand out in more than one.

Specifically, our methods are comparisons of:

- (i) the median differences between the equivalent widths (EWs) in the target stars and in Ceres, for 109 lines covering a range of species and ionisation states (Section 4.2), which is closely related to the “first criterion” method of Meléndez et al. (2006)
- (ii) the relative differences between the EWs of 33 FeI lines in the star and in Ceres, as a function of the excitation potential of the lines (Section 4.3), a method similar to that used by Meléndez & Ramírez (2007)
- (iii) the relative differences in FeI line depths of the same 33 lines, as a function of the excitation potential of the lines (Section 4.4) (the same method as in Meléndez et al. 2006)
- (iv) line depth ratios for specific pairs of high and low excitation potential lines (Section 4.5), a traditional method to derive temperatures (see e.g. Gray & Johanson (1991))

Method (i) makes use of the equivalent widths of 109 lines for 20 elements (kindly provided to us by Ivan Ramírez — private comm.). The lines cover the spectral range of 5000-8000 Å and are carefully selected to be unblended, weak and without telluric contamination. The species measured are OI, NaI, MgI, AlI, SiI, SII, KI, CaI, ScII, TiI, VI, CrI, MnI, FeI+II, CoI, NiI, CuI, ZnI, ZrII and BaII. The median depths of these lines relative to their depths in the comparison solar (Ceres) spectrum are used to search for solar twins.

In Method (ii) and (iii) we confined the twin matching process to the EWs and LDs of just 33 FeI lines (Meléndez et al. 2006). Temperature and metallicity sensitivity in these lines is attained by comparing the median depths of the lines relative to the lines in the Ceres spectrum, as a function of their excitation potential.

Method (iv) uses the line depth (LD) ratios of three pairs of lines very close in wavelength, with one line having a low and one a high excitation potential. This is a classical method to probe temperature, as the line ratios are known to have negligible metallicity sensitivity (as we confirm in section 4.5).

4.1 Measuring equivalent widths and TWOSPEC

We developed a code, TWOSPEC, to measure the equivalent widths of the selected lines. The program compares two spectra at the same time – the target star being analysed and the spectrum of Ceres as the comparison. Equivalent widths are measured simply by computing the missing light in the line in a window 300 mÅ wide, relative to the continuum level in each spectrum. The placement of the two continua in the spectra is an important issue, since we are doing differential spectroscopy between the star and Ceres, thus if the two continua are systematically different, there will also be a systematic difference in the measured equivalent widths. Some well known methods for setting the continuum are to define good continuum regions around each line, or to search for the mode of flux values in the selected window. We choose a third way — we normalise the two spectra by the total flux in each in a 10 Å window around the target line. We achieve two advantages in doing this – since we are searching for stars as similar to the Sun as possible – a perfectly matching spectrum between both the star and Ceres in this window will have the same missing light due to the same lines, and the continuum will be accurately set. For stars which are a slight mismatch to the Sun, the continuum will be commensurately offset, and as this will tend to emphasise the mismatch with the Sun, this aids us in finding good spectroscopic matches. Tests of this procedure show that it works very well. For example, when setting the continuum using the flux normalisation technique, and comparing spectra of the same star HD 147513 to Ceres, yielded a scatter in the measured EWs of 95 lines of 1.4 mÅ (compared to their EWs in Ceres), whereas our best effort to fit the continuum directly resulted in a scatter in the measured EWs for the same 95 lines of 1.9 mÅ relative to Ceres.

TWOSPEC displays to the user both the target and reference spectra centred on the target line, the assigned continuum level, and the window around the line used to measure the EW. The depths of the lines were also measured by estimating the centre of light by fitting a parabola to the three lowest points in the line. We tried Gaussian fitting of the lines to better measure the EWs, but this did not lead to any significant improvement in the EWs – as measured by comparing multiple spectra of the same object – so this technique was not utilised. All lines in all the spectra were inspected by eye by two of us (JD and CF) in this way, allowing us to develop a good impression of the quality of the match for each star, as well as enabling us to drop bad spectra or bad lines due to poor flat fielding, electronic

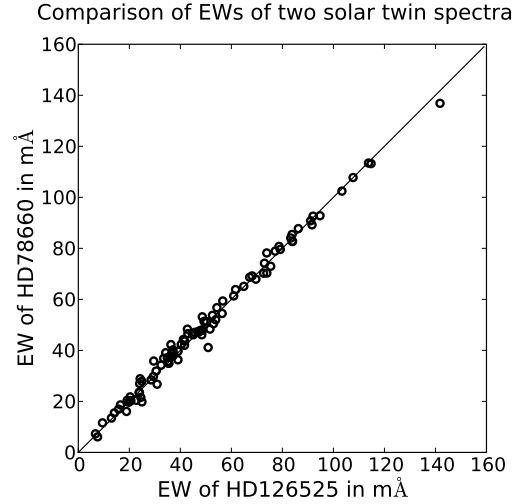


Figure 3. A comparison of measured equivalent widths for the two stars HD 126525 and HD 78660. The line is the 1:1 relation.

readout issues or cosmic rays. TWOSPEC requires no user input beyond viewing the lines individually and confirming that the data are good. Once a few bad spectra had been spotted and dropped, the complete data set could be reduced in batch mode with no user intervention. This made experiments, such as how we set the continuum or measured the EWs or LDs, very straightforward to test.

We also measured EWs by hand for 10 random stars using IRAF. The IRAF and TWOSPEC EWs were found to be in very good agreement, with a scatter of a few mÅ, and no significant systematic offsets.

Fig. 3 shows a comparison of the EWs for the 109 lines of two of our stars, HD 126525 and HD 78660. The lines range in EW from ~10 mÅ to 140 mÅ, with most lines being in the range of 20-80 mÅ.

4.2 Method (i): comparison of EWs for a range of species

This method is closely related to the “first criterion” method of Meléndez et al. (2006). We measured the median $\langle \Delta EW_{\text{all}} \rangle$ and scatter $\chi^2(\Delta EW_{\text{all}})$ of the differences ΔEW_{all} in the EWs of target stars relative to Ceres, for the $N = 109$ lines:

$$\Delta EW_{\text{all}} = (EW(\star) - EW(\odot))/EW(\odot), \quad (1)$$

$$\chi^2(\Delta EW_{\text{all}}) = \sum_{i=1..N} ((EW_i(\star) - EW_i(\odot))/EW_i(\odot))^2, \quad (2)$$

where the solar values refer to the Ceres spectrum.

The results for our 100 stars samples are shown in Fig. 4, plotted as functions of the (GCS-III) temperature and metallicity.

For a solar twin, the median difference $\langle \Delta EW_{\text{all}} \rangle$ vanishes (to within observational error) and $\chi^2(\Delta EW_{\text{all}})$ should be consistent with observational scatter alone. We define solar twins in our method (i) as having $\chi^2(\Delta EW_{\text{all}}) \leq 1$ and a $\langle \Delta EW_{\text{all}} \rangle = 0$ within 2σ . This results in 7 solar twins, and these are listed in Table 1.

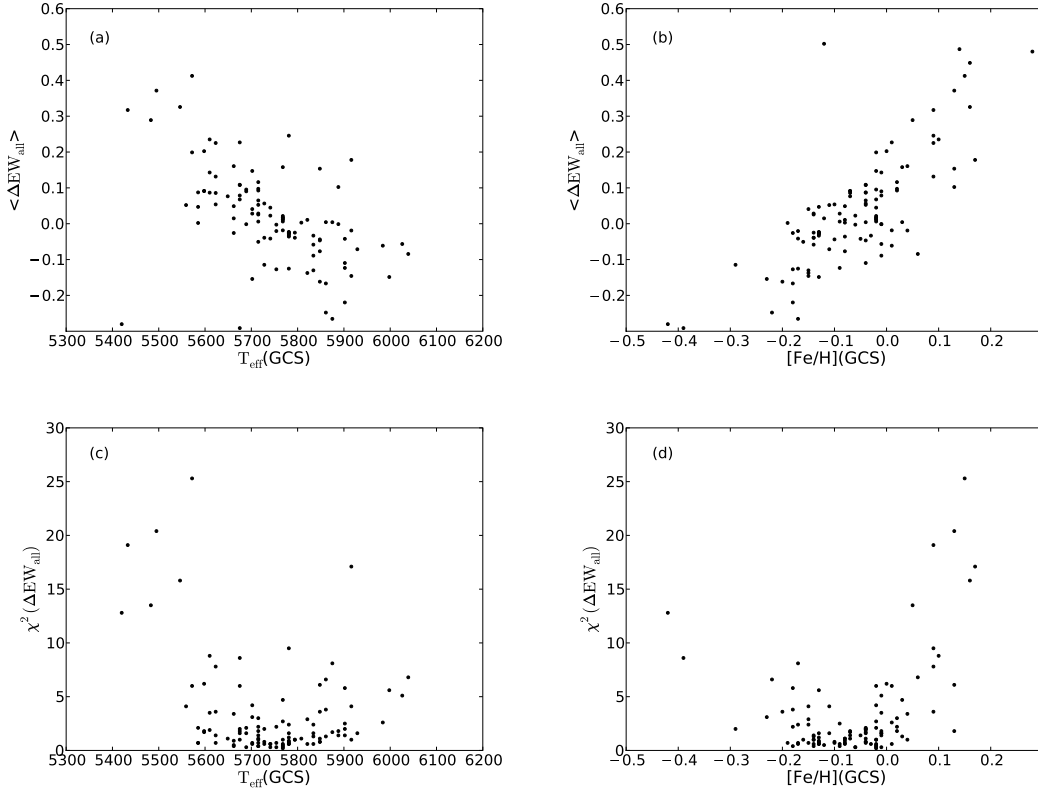


Figure 4. Method (i). Panel (a): Median relative difference of 109 lines of various species in our 100 target stars in comparison to Ceres, plotted as a function of the effective temperature from GCS-III. $\langle \Delta EW_{\text{all}} \rangle$ is anti-correlated with temperature. Panel (b): Same as panel (a), but plotted against the metallicities of the stars from GCS-III. $\langle \Delta EW_{\text{all}} \rangle$ is correlated with $[\text{Fe}/\text{H}]$, as one would expect. Panel (c): Scatter of the relative EWs of the stars compared to Ceres, shown as a function of temperature from GCS-III. The scatter in the relative EWs of the lines increases very rapidly as one moves to cooler or hotter stars relative to the Sun at 5777 K. Panel (d) as for panel (c), but plotted versus the stellar metallicities. The scatter increases rapidly as the stellar metallicities depart from solar in either direction. Note that one can see here already that the scatter is least at a metallicity below the solar value, indicating that the GCS-III metallicity scale might be too metal-poor for solar type stars (as analysed in depth section 5). (We have excluded four stars with high $\chi^2(\Delta EW_{\text{all}})$ for clarity).

Table 1. List of solar twins using $\chi^2(\Delta EW_{\text{all}})$ (i.e. method (i)), ordered by $\chi^2(\Delta EW_{\text{all}})$ (see also Figure 4).

Name	$\chi^2(\Delta EW_{\text{all}})$	$\langle \Delta EW_{\text{all}} \rangle$
HD 146233	0.2 ± 0.4	0.006 ± 0.005
HD 97356	0.3 ± 0.4	-0.003 ± 0.006
HD 138573	0.3 ± 0.4	-0.001 ± 0.006
HD 78660	0.4 ± 0.4	0.006 ± 0.007
HD 117860	0.6 ± 0.4	0.011 ± 0.008
HD 126525	0.7 ± 0.4	0.002 ± 0.009
HD 142415	1.0 ± 0.4	-0.019 ± 0.010

4.3 Method (ii): comparison of FeI equivalent widths versus excitation potential

Method (ii) is based on the technique used by Meléndez & Ramírez (2007). We used only the 33 Fe I lines (from our total list of 109 lines), and computed a new $\langle \Delta EW_{\text{FeI}} \rangle$ as the median of:

$$\Delta EW_{\text{FeI}} = (EW_{\text{FeI}}(\star) - EW_{\text{FeI}}(\odot)) / EW_{\text{FeI}}(\odot) \quad (3)$$

We also measure the slope of the relation between ΔEW_{FeI} and the excitation potential (χ_{exc}) of each Fe I line (see Fig. 5).

Figure 6 shows stars which are good matches to the Sun, where we consider good matches to be stars for which $\langle \Delta EW_{\text{FeI}} \rangle$ and a slope $[\langle \Delta EW_{\text{FeI}} \rangle \text{ vs. } \chi_{\text{exc}}]$ vanishes to within 2σ , where σ is the observational error.

Eight targets satisfy these criteria, and are shown in Table 2 and Fig. 6. Five of these targets are common with the stars found in method (i) – they are HD 78660, HD 117860, HD 126525, HD 138573 and HD 146233.

4.4 Method (iii): comparison of FeI line depths versus excitation potential

In method (iii) we used the same technique as method (ii), but computed the $\langle \Delta LD_{\text{FeI}} \rangle$ (line depth) for the iron lines rather than the EWs (i.e. the exact same technique as in Meléndez et al. 2006):

$$\Delta LD_{\text{FeI}} = (LD_{\text{FeI}}(\star) - LD_{\text{FeI}}(\odot)) / LD_{\text{FeI}}(\odot) \quad (4)$$

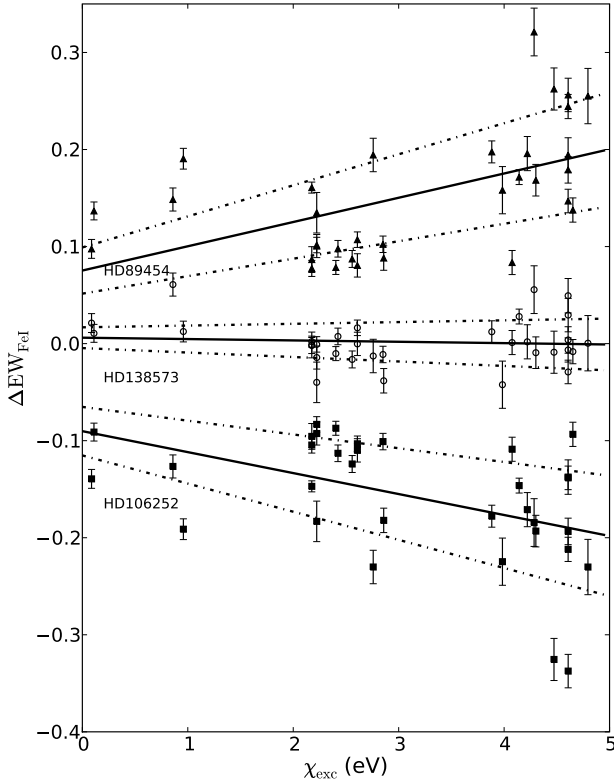


Figure 5. Method (ii). The relative difference in EW of 33 Fe I lines compared to Ceres, plotted as a function of the excitation potential of the lines for three example stars. The solid line shows the least square fit, and the dotted lines are the 1σ error limits, for each star. HD 138573 is an excellent solar twin, having, within observational error, no median difference in the EW of the lines relative to Ceres and no dependence on the excitation potential. For comparison HD 89454 and HD 106252 are poor solar twins, as the EWs of the lines show a clear dependence on excitation potential. The relative difference in EWs and the $\text{slope}[(\Delta\text{EW}_{\text{FeI}}) \text{ vs. } \chi_{\text{exc}}]$ are thus good proxies for the metallicity and temperature of the star relative to the Sun (as extensively discussed by Meléndez et al. 2006 and Meléndez & Ramírez 2007).

Table 2. List of solar twins from method (ii), ordered by name (see also Figure 6).

Name	$\langle\Delta\text{EW}_{\text{FeI}}\rangle$	$\text{slope}[(\Delta\text{EW}_{\text{FeI}}) \text{ vs. } \chi_{\text{exc}}]$
HD 78660	0.007 ± 0.005	0.003 ± 0.008
HD 117860	0.009 ± 0.006	0.012 ± 0.011
HD 126525	0.002 ± 0.005	-0.011 ± 0.011
HD 138573	0.000 ± 0.004	-0.001 ± 0.007
HD 146233	0.000 ± 0.005	0.010 ± 0.006
HD 147513	-0.005 ± 0.005	0.009 ± 0.010
HD 163441	0.005 ± 0.006	0.005 ± 0.009
HD 173071	-0.009 ± 0.010	0.032 ± 0.017

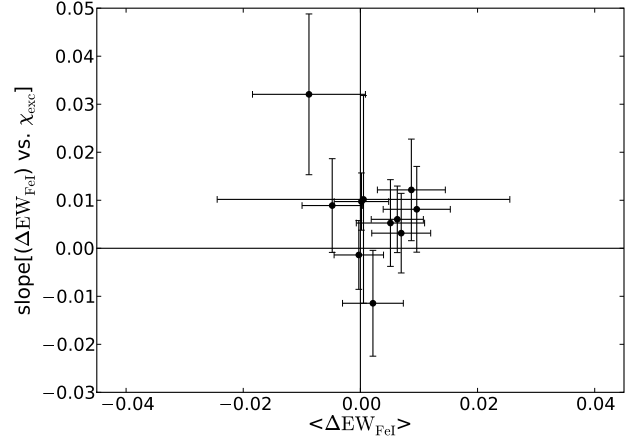


Figure 6. A close-up of the best targets for method (ii). These stars have $\langle\Delta\text{EW}_{\text{FeI}}\rangle$ and $\text{slope}[(\Delta\text{EW}_{\text{FeI}}) \text{ vs. } \chi_{\text{exc}}]$ of 0 within 2σ , here plotted with errorbars of 1σ for clarity.

Table 3. List of solar twins from method (iii), see also Figure 8.

Name	$\langle\Delta\text{LD}_{\text{FeI}}\rangle$	$\text{slope}[(\Delta\text{LD}_{\text{FeI}}) \text{ vs. } \chi_{\text{exc}}]$
HD 126525	-0.005 ± 0.003	-0.004 ± 0.002
HD 146233	-0.025 ± 0.018	0.003 ± 0.013

The slope of the relative line depth differences as a function of the excitation potential of the lines was determined as with method (ii) (Fig. 7).

Our most Sun-like targets are shown in Fig. 8 and are listed Table 3. They are HD 126525 and HD 146233, as they both have indices which vanish to within 2σ . Both stars turn up also in the previous two lists of solar twins.

4.5 Method (iv): Line depth ratios for choice line pairs

This method is based on the technique of Gray & Johanson (1991), who use line depth ratios (LDR) for carefully chosen pairs of lines very close in wavelength to probe excitation temperatures. We used the following pairs: FeI (6089.5 Å)/VI (6090.2 Å); VI (6243.1 Å)/SiI (6243.8 Å) and VI (6251.8 Å)/FeI (6252.6 Å).

We compare the relative difference of these line ratios in the target star and in Ceres, as follows:

$$\Delta\text{LDR} = (\text{LDR}(\star) - \text{LDR}(\odot)) / \text{LDR}(\odot) \quad (5)$$

We show the three ratios as functions of the (GCS-III) temperature of the sample stars in Fig. 9. For each ratio there is a clear temperature dependence, with a scatter that is consistent with the scatter in the GCS temperatures. We found no measurable dependence of the line ratios with metallicity, as expected (Gray & Johanson 1991).

We select solar twins with this method by requiring that the median relative LDR vanishes. Analysis of the LDRs in the stars with repeated spectra show that the typical observational error in the LDR is $\sigma = 0.04$, which we adopt for all stars, given they all have similar S/N. Adopting 2σ limits and using all three line pairs, we confirm four of our

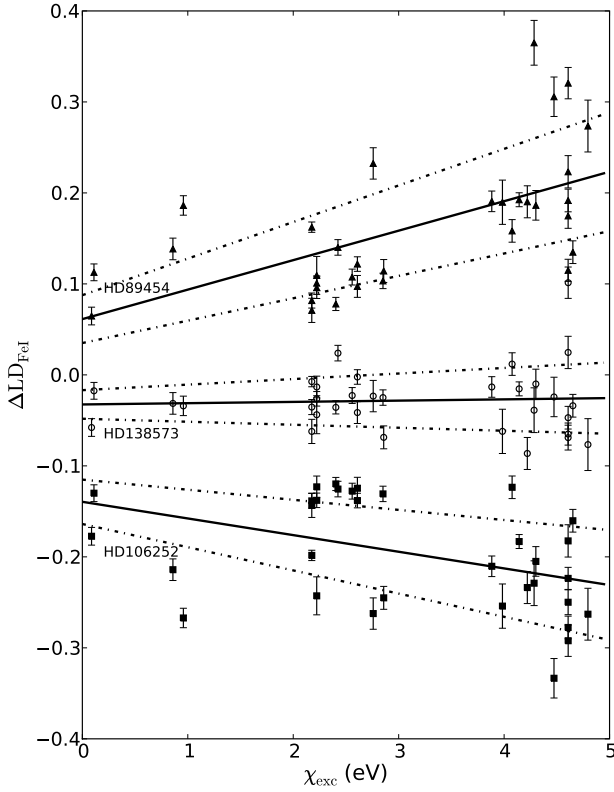


Figure 7. Method (iii) uses the depths of 33 FeI lines in the target star relative to the lines in the Ceres spectrum, and the excitation potential of the lines, to search for solar twins. We show here the the relative difference between the star and Ceres for all 33 FeI lines as a function of excitation potential, for three stars: HD 138573, a very close match to the Sun according to method (iii); and two poor matches to the Sun (HD 89454 and HD 106252).

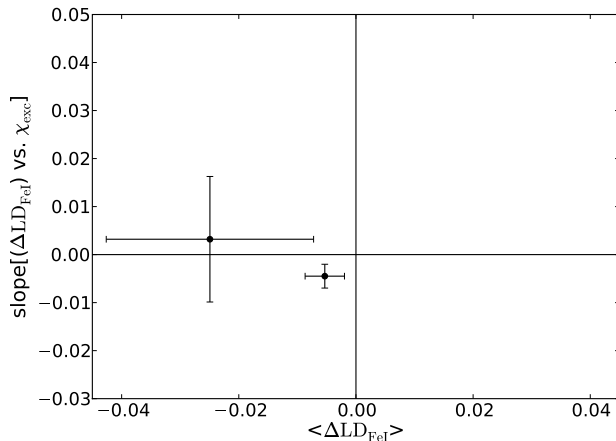


Figure 8. A close-up of the best targets using method (iii). These stars have median $\langle \Delta LD_{\text{FeI}} \rangle$ and $\text{slope}[(\Delta LD_{\text{FeI}}) \text{ vs. } \chi_{\text{exc}}]$ of 0 within 2σ , here plotted with errorbars of 1σ for clarity.

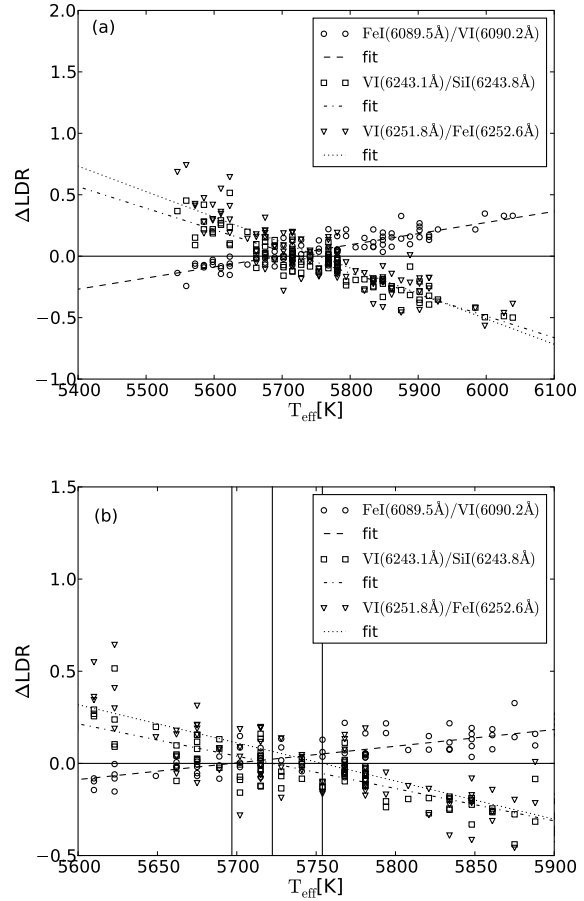


Figure 9. Panel (a): Line depth ratios for the three line pairs, relative to Ceres, shown as a function of GCS temperature and corresponding fits. Panel (b): Same line depth ratios, but zoomed into the temperature range of 5600–5900 K. The vertical black lines guide the eye to the three crossing points with the zero line of the ratios.

Table 4. List of solar twins, confirmed by method (iv)

Name	LDR, using FeI ₆₀₉₀ /VI ₆₀₉₀	LDR, using VI ₆₂₄₃ /SiI ₆₂₄₃	LDR, using VI ₆₂₅₂ /FeI ₆₂₅₃
HD 138573	-0.08 ± 0.04	0.08 ± 0.04	-0.04 ± 0.04
HD 146233	0.02 ± 0.04	0.02 ± 0.04	-0.01 ± 0.04
HD 147513	0.05 ± 0.04	-0.06 ± 0.04	-0.06 ± 0.04
HD 163441	-0.02 ± 0.04	-0.09 ± 0.04	0.09 ± 0.04

previous twin candidates (see Table 4). Since this method is sensitive only to the temperature of the stars, it does not suffice by itself to select solar twins, but needs to be combined with other methods that assess the metallicity. For this reason we used this method only on twins already selected via the other methods, as an additional check on their temperature match to the Sun.

It is clear from Table 4 that HD 146233 (18 Sco) is the best match using method (iv). This star turned up in all four methods, and is certainly our best overall twin.

Table 6. Our solar twins compared to the Sun. Note that the solar ($b - y$) are as estimated indirectly from Sun-like stars by Holmberg et al. (2006). New twins are shown in bold face.

Name	($b - y$)	M_V	[Fe/H] (GCS)	T_{eff} (K) (GCS)	selection method
Sun	0.403	4.83	0.00	5777	
HD 146233	0.404	4.79	-0.02	5768	i, ii, iii, iv
HD 126525	0.426	4.94	-0.19	5585	i, ii, iii
HD 138573	0.413	4.83	-0.10	5689	i, ii, iv
HD 78660	0.409	4.75	-0.09	5715	i, ii
HD 117860	0.393	4.75	-0.08	5821	i, ii
HD 147513	0.397	4.84	-0.13	5781	ii, iv
HD 163441	0.412	4.69	-0.09	5702	ii, iv
HD 97356	0.405	4.69	-0.06	5754	i
HD 142415	0.383	4.66	+0.04	5916	i
HD 173071	0.386	4.54	-0.04	5875	ii

4.6 Multiple spectra and accuracy of the various methods

Thanks to the large selection in the ESO archive, we were able to test the repeatability of our results from multiple spectra of the same target. The best examples are HD 146233 and HD 147513, for which we have six spectra of each target. In Table 5 we show the $\chi^2(\Delta EW_{\text{all}})$, $\langle \Delta EW \rangle$, $\langle \Delta LD \rangle$ and slopes for each spectrum. The spectra were taken in different nights and different years from 2004-2007 and show good agreement in our measurements. The errors for the various measured quantities are: $\sigma(\chi^2(\Delta EW_{\text{all}}))=0.2$, $\sigma(\langle \Delta EW_{\text{all}} \rangle)=0.002$, $\sigma(\langle \Delta EW_{\text{FeI}} \rangle)=0.002$, $\sigma(\text{slope}[(\Delta EW_{\text{FeI}}) \text{ vs. } \chi_{\text{exc}}])=0.001$, $\sigma(\langle \Delta LD_{\text{Fe}} \rangle)=0.004$ and $\sigma(\text{slope}[(\Delta LD_{\text{FeI}}) \text{ vs. } \chi_{\text{exc}}])=0.001$. These error estimates have been adopted throughout section 4, since all stars have spectra of very similar S/N.

4.7 Final list of solar twins

Combining all these approaches and looking at the best twins from all four, HD 146233 is confirmed to be the best twin. We found two other stars, HD 126525 and HD 138573, which satisfied the criteria within the 2σ errors in three of our approaches; although, admittedly, in the case of HD 126525 these errors are rather large, and in fact its parameters are the most extreme (it is a significantly cooler and more metal poor than the Sun according to GCS-III (see Table 6)). Four stars are a match in two criteria, and three are a match in one criterion. All stars satisfying any of our criteria are shown with their stellar parameters (from GCS-III) in Table 6. The new solar twins are identified by being shown in bold face.

In Fig. 10 we illustrate for a small wavelength window (6237 to 6253 Å), how similar our Ceres and solar twin spectra are, by showing their residuals after subtracting the Ceres spectrum. While all the stars are good matches, it is clear that small spectroscopic residuals remain. Note that the vertical lines mark the positions of some of the lines used

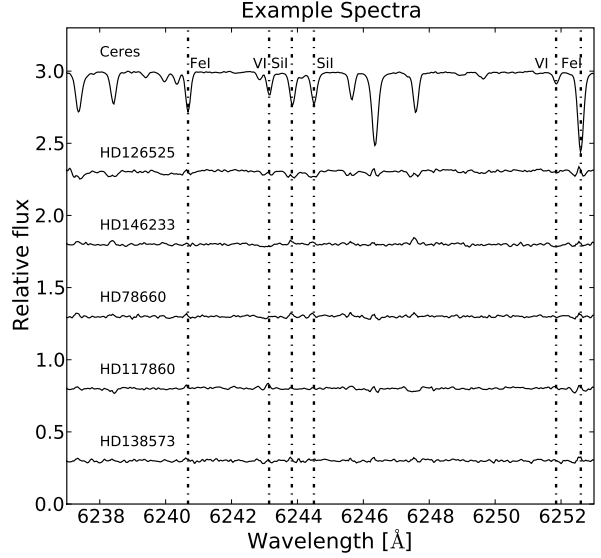


Figure 10. Comparison of the solar spectrum (Ceres) to some of our twins for an example region of the spectrum, including six of our lines (two FeI, two SiI and two VI). Each spectrum is shown as the residual relative to Ceres.

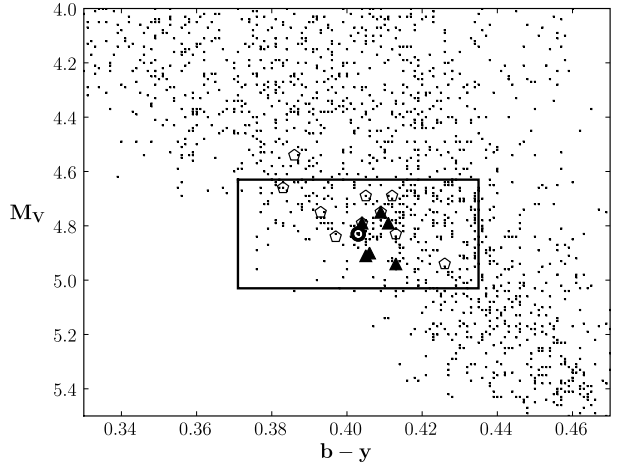


Figure 11. As Figure 1, but showing the locations of our solar twins as open pentagons. Dots show stars from the Nordström et al. (2004) catalogue (GCS-I) and the box is our original selection window. The Sun is marked in the middle of the box, using the ($b - y$) colour estimated indirectly by Holmberg et al. (2006) via solar analogues. The filled triangles show six of 11 solar twins by Meléndez et al. (2009), available in the GCS, for comparison.

for the comparison (FeI, SiI and VI lines) in this particular wavelength window.

Fig. 11 shows the location of these solar twins in the colour magnitude diagram, compared to the original selection window.

Table 5. Comparison of multiple spectra of the same object. Column 1 shows the HD number, and column 2 the spectrum running number. Column 3 and 4 show the results for each spectrum using method (i), columns 5 and 6 for method (ii); and columns 7 and 8 for method (iii) (see section 4.6 for discussion of the typical errors of each method as derived from these multiple spectra.)

Name	Spectrum	$\chi^2(\Delta EW_{\text{all}})$	$\langle \Delta EW_{\text{all}} \rangle$	$\langle \Delta EW_{\text{FeI}} \rangle$	slope $[(\Delta EW_{\text{FeI}}) \text{ vs. } \chi_{\text{exc}}]$	$\langle \Delta LD_{\text{FeI}} \rangle$	slope $[(\Delta LD_{\text{FeI}}) \text{ vs. } \chi_{\text{exc}}]$
HD 146233	1	0.3	0.011	0.006	0.006	-0.057	0.009
HD 146233	2	0.5	0.013	0.010	0.008	-0.050	0.009
HD 146233	3	1.0	0.016	0.015	0.005	-0.039	0.010
HD 146233	4	0.4	0.017	0.011	0.006	-0.043	0.010
HD 146233	5	2.7	0.022	0.001	0.010	-0.025	0.003
HD 146233	6	0.2	0.006	0.000	0.010	-0.056	0.013
HD 147513	1	0.6	-0.026	-0.023	0.006	-0.067	0.015
HD 147513	2	1.2	-0.023	-0.022	0.006	-0.063	0.011
HD 147513	3	1.6	-0.029	-0.021	0.005	-0.066	0.010
HD 147513	4	0.6	-0.024	-0.005	0.009	-0.044	0.016
HD 147513	5	0.8	-0.028	-0.021	0.006	-0.068	0.013
HD 147513	6	0.9	-0.033	-0.020	0.005	-0.067	0.012

4.8 Offset of temperature and metallicity in the solar twins

Table 6 shows that solar twins, proven to be a good match in photometric (chosen in the original sample) as well as spectroscopic quantities (EW and LD of spectral lines) can still be quite different from each other in their individual photometric GCS-III temperatures and metallicities, by up to 200 K and 0.2 dex respectively. The scatter is even larger than the expected errors on individual GCS entries: Nordström et al. (2004) assume typical uncertainties of order 0.1 dex in metallicity and 0.01 dex in $\log T_{\text{eff}}$ (or 135 K, for solar temperatures). This suggests that even the differential spectroscopic criteria used by us (and other authors) for the twin selection, are still affected by metallicity-temperature degeneracy.

This is illustrated in Fig. 12, which shows our solar twins in the GCS-III temperature–metallicity plane. Our twin sample shows a trend towards lower metallicities than the Sun ($T_{\text{eff}} = 5777$ K and $[\text{Fe}/\text{H}] = 0$). In particular, nearly all the twins have sub-solar metallicity, whereas the average twin temperature of 5760 ± 20 K is quite close to the solar T_{eff} . However, especially if temperature–metallicity degeneracies still affect the spectroscopic criteria, the offset in $[\text{Fe}/\text{H}]$ might simply reflect the fact that the peak of the metallicity distribution function in the solar Neighbourhood, in the GCS scale, is around -0.15 dex; which naturally biases the selection toward metal-poor siblings of the Sun. To account for these potential biases, metallicity and temperature for the full sample needs to be fit at the same time (i.e. section 5).

Offsets in the GCS scale, being about 100 K too cool and 0.1 dex too metal-poor, have been suggested by Casagrande et al. (2010), by comparing their Infrared Flux Method scale, to the average values of temperature and metallicity of 10 solar twins from Melendez et al. (2009). For our twins, the average values from Table 6 would suggest a metallicity offset of -0.07 ± 0.01 dex, but a good temperature calibration within 20 K of the Sun.

However, such offsets can hardly be assessed on the basis of only ten stars, even though they are our best solar twins in the sample, considering that the scatter in the twin properties, and the estimated errors on individual entries

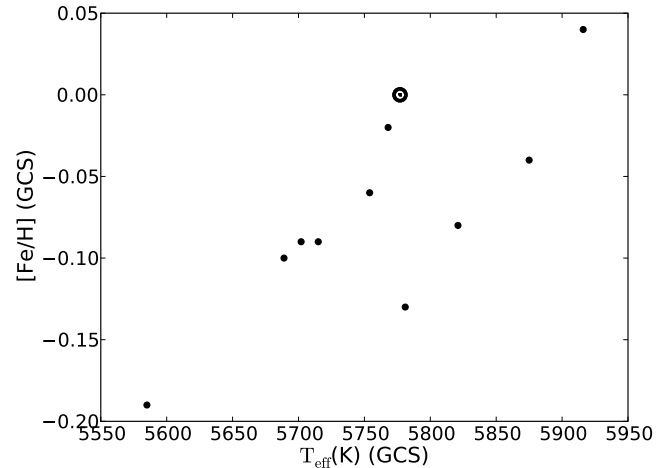


Figure 12. Effective temperatures and metallicities (from GCS-III) of our best solar twins (filled circles), compared to the solar values (dot with circle). There is a trend to lower metallicities than solar in the sample of twins, while the mean temperature is close to the expected value of the Sun of 5777 K.

in the GCS are of the same order or even larger than the offsets. In the next section we therefore devise an alternative method to estimate possible offsets in the GCS scale with a broader approach, which uses our complete sample of Sun-like stars.

5 PROBING THE GCS TEMPERATURE AND METALLICITY SCALE

As mentioned in the previous section, it is difficult to probe any offset in the temperature or metallicity scales of the GCS on the basis of just 10 stars. In this section we use our whole sample of Sun-like stars to test the calibration of the GCS scale, by introducing a new method that relies on the systematic trends in the stellar spectra versus the reference solar/Ceres spectrum.

5.1 The degeneracy lines method

The various quantities ($\langle \Delta \text{EW} \rangle$, $\langle \Delta \text{LD} \rangle$ and corresponding $\text{slope}[(\Delta \text{EW}_{\text{FeI}}) \text{ vs. } \chi_{\text{exc}}]$) measured in our twin search depend both on temperature and metallicity, as can be seen clearly from Fig 4(a) to 4(d). Therefore we solved for this combined dependency by applying 2-D least square fitting of a planar relation of the kind $a[\text{Fe}/\text{H}] + bT_{\text{eff}} + c$, using the GCS values for $[\text{Fe}/\text{H}]$ and T_{eff} .

We used 92 of our stars with temperatures over 5500 K (the hottest being at 6039 K), as we found that below this threshold the dependencies no longer show linearity; this behaviour, that linear fits are only suitable within a limited T_{eff} range, is also confirmed in our test with theoretical spectra in Section 5.3. We have also experimented with narrower temperature ranges around the solar value and verified that the fitting coefficients and the results are quite stable to such changes.

We found the following 2-D planes for our data, with the errors in the fitting coefficients being 5-10%. Note, that the metallicity and temperatures in these planes refer to the GCS values:

$$\langle \Delta \text{EW}_{\text{all}} \rangle = 1.056[\text{Fe}/\text{H}] - 3.829 \frac{T_{\text{eff}} - 5777}{5777} + 0.066 \quad (6)$$

$$\langle \Delta \text{EW}_{\text{FeI}} \rangle = 0.856[\text{Fe}/\text{H}] - 3.769 \frac{T_{\text{eff}} - 5777}{5777} + 0.045 \quad (7)$$

$$\text{slope}[(\Delta \text{EW}_{\text{FeI}}) \text{ vs. } \chi_{\text{exc}}] = 0.256[\text{Fe}/\text{H}] + 0.027 \quad (8)$$

$$\langle \Delta \text{LD}_{\text{FeI}} \rangle = 0.884[\text{Fe}/\text{H}] - 5.348 \frac{T_{\text{eff}} - 5777}{5777} - 0.018 \quad (9)$$

$$\text{slope}[(\Delta \text{LD}_{\text{FeI}}) \text{ vs. } \chi_{\text{exc}}] = 0.248[\text{Fe}/\text{H}] + 0.031 \quad (10)$$

For Eq. 8 and 10 we found empirically that a metallicity dependence suffices to describe the trend, and adding a temperature dependence does not significantly improve the fits (see Fig. 13).

For the Sun, all the quantities on the left hand sides vanish; the fact that the corresponding fitted relations on the right hand sides of Eq. 6-10 do not (as the intercepts are non-zero) already hints to the existence of offsets in the GCS-III temperatures and metallicities to the true solar values. Thus we set the LHS to zero to measure this offset in the temperature and metallicity on the GCS-III scale.

$$[\text{Fe}/\text{H}]_{\langle \Delta \text{EW}_{\text{all}} \rangle} = 3.625 \frac{T_{\text{eff}} - 5777}{5777} - 0.062 \quad (11)$$

$$[\text{Fe}/\text{H}]_{\langle \Delta \text{EW}_{\text{FeI}} \rangle} = 4.406 \frac{T_{\text{eff}} - 5777}{5777} - 0.053 \quad (12)$$

$$[\text{Fe}/\text{H}]_{\text{slope}[(\Delta \text{EW}_{\text{FeI}}) \text{ vs. } \chi_{\text{exc}}]} = -0.106 \quad (13)$$

$$[\text{Fe}/\text{H}]_{\langle \Delta \text{LD}_{\text{FeI}} \rangle} = 6.052 \frac{T_{\text{eff}} - 5777}{5777} + 0.021 \quad (14)$$

$$[\text{Fe}/\text{H}]_{\text{slope}[(\Delta \text{LD}_{\text{FeI}}) \text{ vs. } \chi_{\text{exc}}]} = -0.124 \quad (15)$$

These relations correspond to (empirical) *degeneracy lines*, along which the condition $\langle \Delta \text{EW} \rangle = 0$, $\text{slope} = 0$ etc. are respectively maintained. A star which may differ in metallicity and temperature to the Sun, will have the same measured spectroscopic indices as the Sun, along these lines of temperature-metallicity degeneracy. We have five such relations, but they differ in their metal and temperature dependence, allowing us to disentangle the degeneracies.

In Fig. 14 we plot these 5 relations in the GCS

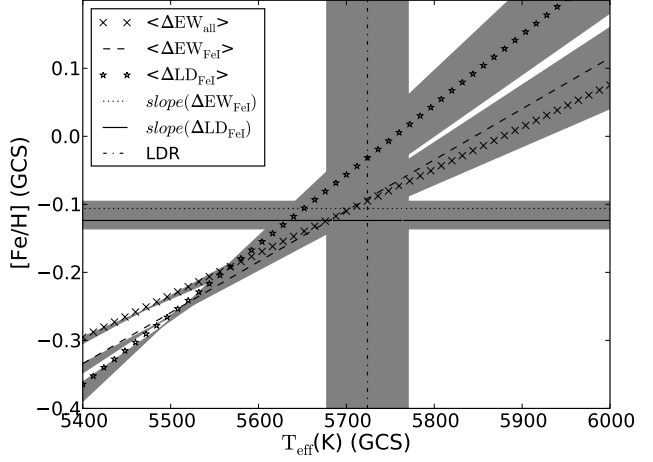


Figure 14. Derived relations for the various measured indices in the GCS-III temperature–metallicity plane. Grey areas mark the uncertainties in the fits. The solar values of the GCS scale are estimated to lie where the lines converge. We estimate this to lie at a metallicity of ~ -0.12 dex and a temperature of approximately 5680 K, providing evidence that the GCS-III metallicity and temperature scales are shifted by about 0.1 dex and 100 K from the Sun.

temperature–metallicity plane, also including the solar temperature range we get from the LDR measurements, see Fig. 9(b).

As mentioned above, the solar values of metallicity and temperature lie where all degeneracy lines would ideally cross, representing a simultaneous zero–point for all of the relations above. There is no such single crossing point, but we estimate the solar values to lie where the horizontal lines (slopes) cross the inclined lines (Δ). Thus the solar zero–point lies around a GCS temperature of $T_{\text{eff}} = 5680 \pm 40$ K and a metallicity of $[\text{Fe}/\text{H}] = -0.12 \pm 0.02$. This corresponds to an offset in the GCS-III scale of about $\Delta T = -100$ K and $\Delta[\text{Fe}/\text{H}] = -0.1$ dex with respect to the true solar values, meaning the GCS scale seems to be too cold and too metal poor, at least around the solar temperature. This confirms the findings of Casagrande et al. (2010), who found similar offsets.

The offsets we quote are based on the various spectroscopic quantities relevant for methods (i)–(iii) of Section 4. We note that method (iv), which is only sensitive to temperature, yields a smaller but still non-negligible offset of about -50 K in the temperature scale of GCS-III (see Fig. 14).

5.2 The solar (b – y) colour

We applied an analogous procedure to the previous section, using the (b – y) colour instead of temperature to get an estimate of this colour for the Sun. The results are shown in Fig. 15. We estimate a solar (b – y) colour of 0.414 ± 0.007 , which on is in good agreement with the very precise value by Meléndez et al. (2010) of 0.411 ± 0.002 , but is in mild tension with our initially assumed value in selecting the sample of solar twin candidates (i.e. 0.403 ± 0.013 ; Holmberg et al (2006)). The initial colour selection window was much

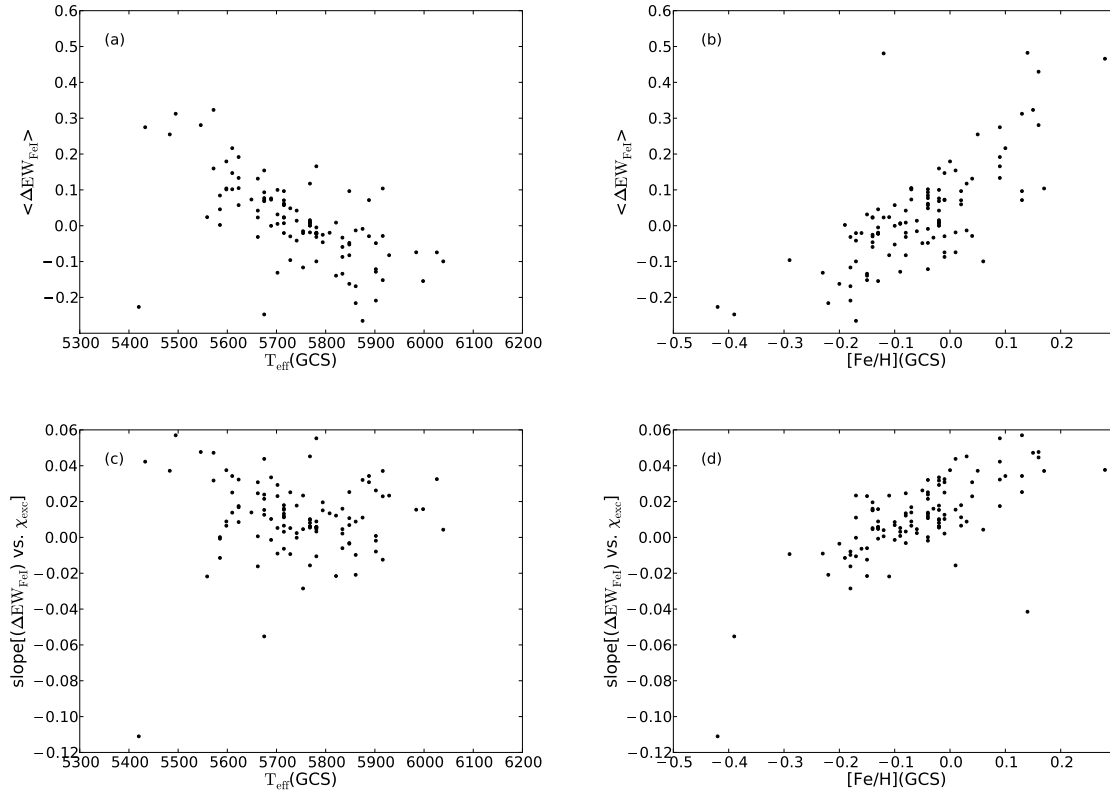


Figure 13. For method (ii) (section 4.3), we show in panel (a) and (b) the dependencies of $\langle \Delta EW_{\text{FeI}} \rangle$ on temperature and metallicity. In Panel (c) and (d), the same for slope[(ΔEW_{FeI}) vs. χ_{exc}]. We find no correlation of the slope with temperature. Planar fits of the form $a[\text{Fe}/\text{H}] + bT_{\text{eff}} + c$ to the measured quantities allow us to solve for effective temperature and metallicity of the Sun in the GCS-III (section 5).

wider than this small change to the colour, so this is very unlikely to have biased the sample.

This procedure yields another estimate for the metallicity of a solar twin on the GCS-III scale: we get $[\text{Fe}/\text{H}] = -0.11 \pm 0.01$. This is in good agreement with the result in the previous section.

5.3 Testing the method : internal precision and synthetic spectra

The method of solving for the crossing points of differing temperature and metallicity degeneracy relations is novel, so we have performed a number of tests to validate that it returns the required results.

Our first test was to use the method on randomly chosen reference stars in the data set, rather than the Ceres spectrum. We ran the same routines and used the same approach to determine the crossing point of the degeneracy lines as described in section 5.1. This tests whether the temperature and metallicities of the reference star can be recovered within the GCS scale. We found that our method indeed recovers the GCS temperatures and metallicities very well: comparing the recovered temperatures and metallicities to GCS values of the reference star, we get typical offsets of $\Delta T = 24\text{ K}$ with a scatter of 50 K, and $\Delta[\text{Fe}/\text{H}] = 0.00$ with a scatter of 0.06 dex. These are small compared to the offsets we find between the Ceres spectrum and the GCS scale,

Table 7. Tests of the degeneracy relations method. Column 1 shows the reference star, and columns 2 and 3 its GCS temperatures and metallicities. Columns 4 and 5 show the values recovered from our degeneracy line fitting, by comparing the reference star to the rest of the sample stars.

Name	GCS T_{eff}	GCS $[\text{Fe}/\text{H}]$	recovered T_{eff}	recovered $[\text{Fe}/\text{H}]$
HD 12264	5728	-0.14	5733	-0.11
HD 78660	5715	-0.09	5608	-0.10
HD 126525	5585	-0.19	5538	-0.19
HD 138573	5689	-0.10	5616	-0.15
HD 155968	5662	0.04	5683	0.07
HD 222669	5834	-0.03	5846	-0.05

of $\approx 100\text{ K}$ and 0.1 dex. In no case do we find a *combined* error on the recovered temperature and metallicity as large as what we find for Ceres; hence we are confident that the GCS offsets are real. Table 7 summarises some results from this test.

As a final check on our method in section 5.1, we applied it to a set of synthetic spectra of Sun-like stars. The spectra were taken from the ‘‘Grids of ATLAS9 Model Atmospheres and MOOG Synthetic Spectra’’ computed by Kirby (2011), and available from the VizieR On-line Data Catalog (Catalog code VI/134) at

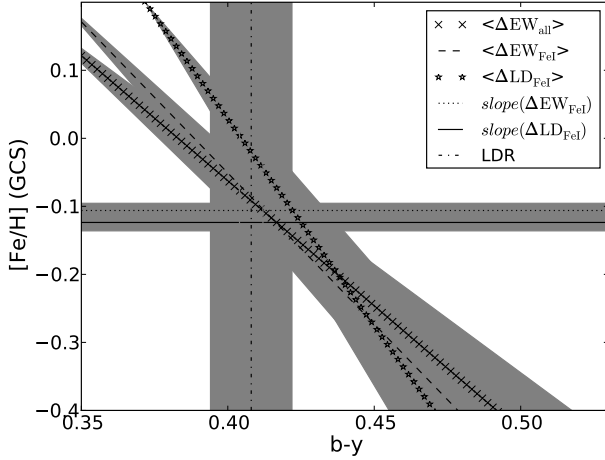


Figure 15. Degeneracy lines between metallicity and temperature for the quantities in the various methods in section 4, shown in the $(b - y)$ –metallicity plane; the solar values lie where the degeneracy relations converge. We estimate a solar $(b - y)$ of 0.414 ± 0.007 from this plot, in good agreement with the recent estimate by Meléndez et al. (2010) of 0.411 ± 0.002 .

SIMBAD (<http://simbad.u-strasbg.fr/simbad/>). The spectra have been computed using MOOG (Snedden 1973), and cover the grid $3500 \text{ K} \leq T_{\text{eff}} \leq 8000 \text{ K}$, $0.0 \leq \log g \leq 5.0$, $-4.0 \leq [M/H] \leq 0.0$, and $-0.8 \leq [\alpha/\text{Fe}] \leq +1.2$, in the wavelength range 6300 \AA to 9100 \AA , with a resolution of 20 m\AA , slightly better than that in our data (30 m\AA). Around the Sun, spectra are available in the library at $[Fe/H] = -0.2, -0.1$ and 0.0 and ($T_{\text{eff}} = 5500, 5600, 5800, 6000$ and 6200 K). We selected spectra for which $\log g = 4.5$ as representative of main sequence stars, and $[\alpha/\text{Fe}] = 0.0$, as alpha enhancement in this metallicity range is mild, and our lines are mainly due to Fe. This resulted in 15 synthetic spectra very similar to our observational spectra in their basic stellar properties. Our line list contains 95 lines in the range 5044 \AA to 7836 \AA , but most of the lines are blueward of the lower wavelength cutoff of 6300 \AA of the theoretical spectra, so that we only had 27 lines left after taking this into account. We measured equivalent widths for these 27 lines in the synthetic spectra using TWOSPEC, using the spectrum at $T_{\text{eff}} = 5800 \text{ K}$ and $[Fe/H] = 0.0$ as our reference spectrum, and applied our basic method to the results. The library spectra are noise-free, and we sampled them with a signal to noise (conservatively) of 100:1.

Doing this we get 5814 K and 0.012 dex for the reference spectrum, compared to the input values of 5800 K and 0.000 dex . Fitting to just the temperature range 5600 to 6000 K , we recover a temperature and metallicity of 5803 K and 0.004 dex , so the choice of temperature and metallicity range have only a small effect on the solutions. Interestingly, sampling the theoretical spectra with a signal to noise of only 20:1, we recover an effective temperature and metallicity for the reference spectrum of 5800 K and -0.01 dex , demonstrating that the method is robust to spectra of rather poor quality.

Some time after completing the MOOG study above, we found a much more extensive library of spectra, both

in metallicity and temperature coverage, as well as spectral coverage, in the Pollux spectral library (Palacios et al. 2010). The spectra also have 20 m\AA resolution and cover our full wavelength range of analysed lines.

Sixty grid points around a "Solar" model at $T_{\text{eff}} = 5750 \text{ K}$, $\log g = 4.5$ and $[Fe/H] = 0.0$ were selected from the library, at grid points of $T_{\text{eff}} = 5500, 5750, 6000$ and 6250 K , and metallicities of $-0.5, -0.25, 0.0, 0.25$ and 0.5 . We applied the same method as used on the MOOG spectra but now with a much larger line list because of the full spectral coverage, and inserted similar noise as in our real spectra. We fully confirm our findings with the MOOG spectra, that the method recovers the correct temperature (within 30 K) and metallicity (within 0.02 dex) of the reference star.

These studies of synthetic spectra offer substantial support for our basic methodology, showing we can recover the temperature and metallicity of reference stars from a sample of stars with similar metallicities and temperatures. We could improve the analysis substantially by using a much finer grid of temperatures, spaced by 50 K instead of 100 to 200 K . This would involve computing dedicated spectra, rather than drawing from a pre-computed library, and we leave this to future work.

6 SUMMARY AND CONCLUSIONS

In this paper we use high resolution optical spectroscopy to search for solar twins in the Geneva Copenhagen Survey, by applying various methods adopted from recent literature. We have shown that there is no unique way to search for a solar twin and that it is necessary to include photometric as well as spectroscopic selection criteria to really determine which stars are solar twins.

We confirm HD 146233 (18 Sco) as the best twin in our list, being selected by all 4 spectroscopic methods used; HD 126525 and HD 138573 are second best, being selected in 3 out of 4 methods; 6 out of our 10 twins are new additions to the literature; HD 117860, HD 97356, HD 142415, HD 163441, HD 173071 and HD 126525.

We use our entire sample to probe for offsets in the temperature and metallicity scale in the GCS for Sun-like stars, introducing a new method (degeneracy lines method) which disentangles the differing metallicity and temperature degeneracies in the measured indices for our stars.

We estimate that, for Sun-like stars, the GCS-III scale is offset by $(-0.12 \pm 0.02) \text{ dex}$ and $(-97 \pm 35) \text{ K}$ respectively – i.e. we find it is a little too metal poor and cool. This result is in good agreement with similar offsets claimed in recent literature, based on solar twins: Meléndez et al. (2010) find the GCS values to be $\Delta T = 48 \text{ K}$ too cool and $\Delta[Fe/H] = 0.09$ too metal poor. Casagrande et al. (2010) finds offsets of about -100 K and -0.1 dex , respectively.

Our new method has been successfully tested both internally in GCS (i.e. recovering the metallicity and temperature of random reference stars, which replaced the Sun/Ceres for the sake of the test) and on theoretical spectra. We are currently applying a similar degeneracy lines method to the very high quality High Accuracy Radial velocity Planet Searcher (HARPS) archive spectra, using both neutral and ionised species for more elements than just Fe. Early results confirm the offsets found here and will be dis-

cussed in a forthcoming paper (Datson et al., in preparation).

Despite the agreement of our results with other studies for an offset in the temperature and metallicity scales of GCS for Sun-like stars, we point out that recent measurements of the temperatures of Sun-like stars via interferometry with the Center for High Angular Resolution Astronomy (CHARA) array instrument (Boyajian et al. 2012) show, for over a dozen stars with the most secure angular diameters (>1 mas) *excellent agreement* with GCS temperatures (Holmberg, private comm.). This contrasts with the conclusions drawn by us and other authors, based on solar twins and Sun-like stars. We leave the discussion of this intriguing result to future work.

The offsets we find in the GCS would imply the solar ($b - y$) colour to be $(b - y) = 0.414 \pm 0.007$, also determined via our degeneracy-lines approach. This colour is redder than the $(b - y) = 0.403 \pm 0.013$ found earlier by our group (Holmberg et al. 2006) but very close to the recent result of Meléndez et al. (2010), based on solar twins.

One of our best solar twins, HD 126525, has a temperature and metallicity, that are so offset from solar (5585 K and -0.19 dex, see Table 6), that even the proposed corrections to the GCS scale still leave it in tension with the solar values. We cannot rule out that the twin selection methods used here are still affected by systematics; a more detailed study of the individual spectra and of metallicity-temperature degeneracy issues is currently underway.

Three of our twins are known to host an exoplanet: HD 142415, HD 147513 (Mayor et al. 2004) and HD 126525 (Mayor et al. 2011). There have been no confirmed detections of exoplanets for the other seven twins so far, which will hopefully be included as targets for future planet searches.

ACKNOWLEDGMENTS

We would like to thank Johan Holmberg for insightful and constructive criticism on our work; Ivan Ramírez and Jorge Meléndez for useful discussions; A. Mueller, B. Conn, A. Ederoclite and the anonymous ESO staff observers, for the data acquisition at the telescope. We would also like to thank the referee for thorough reading and very constructive criticisms. This research has made use of the SIMBAD database, operated at CDS, Strasbourg, France.

This study was financed by the Academy of Finland (grant nr. 130951 and 218317) and the Beckwith Trust. We thank the University of Sydney and Swinburne University, where part of this work was carried out.

REFERENCES

- Allen, C. W., 1976, *Astrophysical Quantities*, London: Athlone (3rd edition)
- Asplund, M., Grevesse, N., Sauval, A. J. and Scott, P., 2009, *ARA&A*, 47, 481
- Bazot, M., Ireland, M. J., Huber, D., Bedding, T. R., Broomhall, A.-M., Campante, T. L., Carfantan, H., Chaplin, W. J., Elsworth, Y., Meléndez, J., Petit, P., Théado, S., van Grootel, V., Arentoft, T., Asplund, M., Castro, M., Christensen-Dalsgaard, J., Do Nascimento, J. D., Dintrans, B., Dumusque, X., Kjeldsen, H., McAlister, H. A., Metcalfe, T. S., Monteiro, M. J. P. F. G., Santos, N. C., Sousa, S., Sturmann, J., Sturmann, L., Ten Brummelaar, T. A., Turner, N. and Vauclair, S., 2011, *A&A*, 526, 4
- Boyajian, T. S., McAlister, H. A., van Belle, G., et al. 2012, *ApJ*, 746, 101
- Casagrande, L., Ramírez, I., Meléndez, J., Bessell, M. and Asplund, M., 2010, *A&A*, 512, A54
- Cayrel de Strobel, G., 1996, *A&A Rev.*, 7, 243
- Endl, M., Cochran, W. D., Hatzes, A. P. and Wittenmyer, R. A., 2005, *RMxAC*, 23, 64
- Gray, D. F. and Johanson, H. L., 1991, *PASP*, 103, 439
- Hall, J. and Lockwood, G. W., 2000, *ApJ*, 545, L43
- Hall, J. C., Henry, G. W., Lockwood, G. W., Skiff, B. A. and Saar, S. H., 2009, *AJ*, 138, 312
- Holmberg, J., Flynn, C. and Portinari, L., 2006, *MNRAS*, 367, 449
- Holmberg, J., Nordström, B. and Andersen, J., 2007, *A&A*, 475, 519
- Holmberg, J., Nordström, B. and Andersen, J., 2009, *A&A*, 501, 941
- Kaufer, A., Stahl, O., Tubbesing, S., Norregaard, P., Avila, G., Francois, P., Pasquini, L., and Pizzella, A. 1999, *The Messenger* 95, 8.
- King, J. R., Boesgaard, A. M. and Schuler, S. C., 2005, *AJ*, 130, 2318
- Kirby, E. N., 2011, *PASP*, 123, 531
- van Leeuwen, F., 2007, *A&A*, 474, 653
- Mayor, M. and Queloz, D., 1995, *Nature*, 378, 355
- Mayor, M., Udry, S., Naef, D., Pepe, F., Queloz, D., Santos, N. C. and Burnet, M., 2004, *A&A*, 415, 391
- Mayor, M. et al., 2011, preprint (arXiv:1109.2497)
- Meléndez, J., Dodds-Eden, K. and Robles, J., 2006, *ApJ*, 641, L133
- Meléndez, J. and Ramírez, I., 2007, *ApJ*, 669, L89
- Meléndez, J., Asplund, M., Gustafsson, B., and Yong, D., 2009, *ApJ*, 704, L66
- Meléndez, J., Schuster, W. J., Silva, J. S., Ramírez, I., Casagrande, L. and Coelho, P., 2010, *A&A*, 522, A98
- Nordström, B., Mayor, M., Andersen, J., Holmberg, J., Pont, F., Jørgensen, B. R., Olsen, E. H., Udry, S. and Mowlavi, N., 2004, *A&A*, 418, 989
- Önehag, A., Korn, A., Gustafsson, B., Stempels, E. and VandenBerg, D. A., 2011, *A&A*, 528, A85
- Palacios, A., Gebran, M., Josselin, E., Martins, F., Plez, B., Belmas, M. and Lebre, A., 2010, *A&A*, 516, A13
- Porto de Mello, G. F. and da Silva, L., 1997, *ApJ*, 482, L89
- Ramírez, I., Meléndez, J. and Asplund, M., 2009, *A&A*, 508, L17
- Snedden, C. A., 1973, PhD thesis, Univ. Texas at Austin
- Soubiran, C. and Triaud, A., 2004, *A&A*, 418, 1089
- Sousa, S. G., Santos, N. C., Israelian, G., Mayor, M. and Monteiro, M. J. P. F. G., 2006, *A&A*, 458, 873
- Takeda, Y., Sato, B., Kambe, E., Sadakane, K. and Ohkubo, M., 2002, *PASJ*, 54, 1041
- Takeda, Y., Kawanomoto, S., Honda, S., Ando, H. and Sakurai, T., 2007, *A&A*, 468, 663
- Udry, S. and Santos, N. C., 2007, *ARA&A*, 45, 397

This paper has been typeset from a \TeX / \LaTeX file prepared by the author.